A spectral model for transient heat flow in a double U-tube geothermal heat pump system

Al-Khoury, Rafid; Focaccia, Sara

Important note
To cite this publication, please use the final published version (if applicable).
Please check the document version above.

A Spectral Model for Transient Heat Flow in a Double U-tube Geothermal Heat Pump System

Rafid Al-Khoury[1] and Sara Focaccia[2]

[1]Faculty of Civil Engineering and Geosciences, Computational Mechanics, Delft University of Technology, P.O. Box 5048, 2600 GA Delft, The Netherlands

[2]CERENA- Centre for Natural Resources and the Environment, Instituto Superior Técnico, Lisbon Technical University, Av. Rovisco Pais 1, 1049-001 Lisbon, Portugal

Abstract

This paper introduces a semi-analytical model based on the spectral analysis method for the simulation of transient conductive-convective heat flow in an axisymmetric shallow geothermal system consisting of a double U-tube borehole heat exchanger embedded in a soil mass. The proposed model combines the exactness of the analytical methods with an important extent of generality in describing the geometry and boundary conditions of the numerical methods. It calculates the temperature distribution in all involved borehole heat exchanger components and the surrounding soil mass using the fast Fourier transform, for the time domain; and the complex Fourier and Fourier-Bessel series, for the spatial domain. Numerical examples illustrating the model capability to reconstruct thermal response test data together with parametric analysis are given. The CPU time for calculating temperature distributions in all involved components, pipe-in, pipe-out, grout, and soil, using 16,384 FFT samples, for the time domain, and 100 Fourier-Bessel series samples, for the spatial domain, was in the order of 3 seconds in a normal PC. The model can be utilized for forward calculations of heat flow in a double U-tube geothermal heat pump system, and can be included in inverse calculations for parameter identification of shallow geothermal systems.

Keywords: Borehole heat exchanger, GSHP, TRT, spectral analysis, FFT.

1. Introduction

Geothermal heat pump (GHP) is an important source of energy for heating and cooling of buildings. It saves energy by making use of the relatively constant temperature conditions at small depths of the earth. This system, also known as borehole heat exchanger (BHE) or ground source heat pump (GSHP), works by circulating a fluid (refrigerant), mostly water with antifreeze solution, through a closed loop of polyethylene pipe that is inserted in a borehole in a soil mass. The borehole is filled with some grouted materials to fix the polyethylene pipe and to ensure a good thermal interaction with the soil. Several types of GHP are available in practice. In this publication, the GHP system is assumed to consist of a vertical double U-tube BHE embedded in a soil mass and subjected to an inlet temperature coming from the heat pump, air temperature, and a temperature coming from the bottom of the earth.

The borehole heat exchanger is a slender heat pipe with dimensions of the order of 30 mm in diameter for the U-tube, and 150 mm in diameter and 100 m in length for the borehole. The U-tube carries a working (circulating) fluid that collects heat from the surrounding soil via convection-conduction heat flow mechanisms. Physically, the heat flow process in such a system is well understood, but computationally, and in spite of the bulk of existing models, still creeping due to the combination of the slenderness of the boreholes heat exchangers and the involved thermal convection. This combination constitutes the main source of computational challenges in this field. Consequently, several theoretical and computational assumptions and approximations have been introduced in order to circumvent this problem and obtain feasible solutions. All

Corresponding author: Rafid Al-Khoury. Tel.: +31-152788744, e-mail: r.i.n.alkhoury@tudelft.nl

known solution techniques, such as analytical, semi-analytical and numerical, have been utilized for this purpose. However, in spite of the versatility of the numerical methods, analytical and semi-analytical solutions are yet preferable because of their comparatively little demands on computational power and ease of use in engineering practice. In this publication, focus is placed on analytical and semi-analytical solution techniques.

In the last three decades, several analytical and semi-analytical models for the simulation of heat flow in geothermal heat pump systems with different complexities and rigor have been introduced. Based on their treatment of heat flow inside the U-tubes, these models can be classified into three categories: 1. No heat convection; 2. Implicit convection; and 3. Explicit convection.

Models belonging to the first category are those based on the work of Carslaw and Jaeger [1], who seem to be the first to introduce a comprehensive treatment of heat conduction in solids. Heat flow in finite, semi-infinite and infinite domains subjected to point, line, plane and cylindrical heat sources were extensively studied in their work between 1947 and 1959. In the meanwhile, and on the basis of Carslaw and Jaeger work, Ingersoll et al. [2] made a significant contribution to the field of heat conduction in solids and provided a practical framework for modeling geothermal systems. Currently, most of the analytical and semi-analytical models for heat flow in geothermal heat pumps are based on these two sources. These models calculate heat flow in a soil mass subjected to a heat source, representing the borehole heat exchanger, regardless of the convective heat flow in the fluid inside the U-tubes and the thermal resistance between the different components. Philippe et al. [3] gave a perceptive review of these models and the researchers who employed them.

Along the same category, but different representation of the geometry, there are several other models in use. In such models, the convective-conductive heat flow in the U-tubes is replaced by a constant cylindrical heat source, and the geometry is described by a concentric two-dimensional (radial) composite domain. Gu and O'Neal [4] gave an elaborate literature review on analytical solutions of radial heat conduction in a composite domain. They utilized this technique to simulate transient heat flow due to a constant heat source, resembling U-tubes, surrounded by a backfill (grout) and a soil mass bounded by a far field boundary. The cross sectional areas of the two branches of the U-tubes are replaced by an equivalent cross sectional area. They utilized the eigenfunction expansion to solve the governing partial differential equation that gave rise to solving an eight degree transcendental equation for determining the involved eigenvalues. Apparently, solving an eight degree transcendental equation is difficult and might be a source of numerical oscillations and computational inefficiency. In this model, summing up to 1000 terms was needed for the series to converge.

Based on Gu and O'Neal's approach, a number of models have been introduced using different mathematical formulations and solution techniques. Lamarche and Beauchamp [5] solved Gu and O'Neal's composite problem using Laplace transform. They solved both forward and inverse Laplace transforms analytically. Bandyopadhyay et al. [6] solved the same problem using dimensionless equations by means of Laplace transform. They utilized Gaver-Stehfest numerical algorithm to solve the inverse Laplace transform. Such models, together with those employing the finite, infinite and cylindrical line sources, can also be classified as a no thermal resistance models.

Models belonging to the second category are those which calculate the BHE fluid temperature implicitly, i.e. without really simulating fluid flow along the axial axis of the U-tubes. In such models, a mean fluid temperature is specified to indicate the average temperature in the U-tubes. It is calculated by first computing the soil temperature at the borehole wall, using any of the known analytical models, then adjusting the borehole thermal effective resistance to obtain equilibrium. Marcotte and Pasquier [7] introduced such a model for a transient pseudo convective

problem using the fast Fourier transform for discretizing the time domain, and the cubic spline for interpolating results obtained at selected samples of the analytical function. They utilized the principle of superposition method to simulate the response to multiple heat fluxes. Javed and Claesson [8] solved Gu and O'Neal's problem using a similar pseudo convective approach.

Yet another type of models has also been introduced that implicitly accounts for the fluid heat flow in the U-tubes. In this kind of models, heat flow in a geothermal heat pump is described by an assembly of interconnected resistances and capacitors. De Carli et al. [9] and Zarrella et al. [10] proposed what is known as the Capacity Resistance Model (CaRM) for the calculation of transient temperature distributions in borehole heat exchangers, including those for the grout and the circulating fluid. In this model, the geometry is discretized by nodes representing slices in the vertical and radial directions. Heat flow in a slice is described by calculating the temperature difference between adjacent slices, controlled by the thermal resistance between them. Bauer et al. [11] extended the idea of the CaRM model by dividing the grout thermal resistance over the number of the involved U-tubes in the borehole. Their model is known as the Thermal Resistance Capacity Model (TRCM). Pasquier and Marcotte [12] extended Bauer et al. [11] model by incorporating the circulating fluid and the pipe thermal capacity. They also introduced a better account for the pipe spacing. This kind of models, and in spite of their apparent ease of formulation, is sensitive to the number of nodes utilized to discretize the geometry, making them sensitive to the thermal parameters, the definition of thermal resistance and the time steps. Such models can also be classified as thermal resistance models.

Models belonging to the third category are those which calculate the BHE fluid temperature explicitly, i.e. simulating fluid flow along the axial axis of the U-tubes. Eskilson and Claesson [13] introduced a semi-analytical model for ground source heat pumps that approximates heat flow in the borehole heat exchangers by two interacting channels conveying a circulating fluid in the vertical axis and embedded in an axisymmetric soil mass. Heat flow in the channels is assumed steady state convective, and in the soil, transient conductive. They utilized Laplace transform to solve the involved heat equations of the channels, and the explicit forward difference method to solve the heat equations of the soil mass. Zeng et al. [14] solved the same problem but using dimensionless heat equations for the channels. This kind of models, in spite of its realistic physical representation of heat flow in the GHP system, is mainly suitable for long term analyses. As for the second category models, this kind of models can also be classified as thermal resistance models.

Alongside this category, Al-Khoury [15,16] introduced a semi-analytical model for transient conductive-convective heat flow in a single U-tube borehole heat exchanger embedded in a soil mass. The model calculates the temperature distribution in all involved borehole heat exchanger components (pipe-in, pipe-out and grout), and the surrounding soil mass using eigenfunction expansion in terms of the spectral analysis method. The fast Fourier transform is utilized for discretizing the time domain, and the complex Fourier series and Fourier-Bessel series are utilized for discretizing the spatial domain. The main advantage of this model is that it solves the governing partial differential equations of the system directly, making it physically sound. Additionally, the use of the spectral analysis makes it computationally efficient.

In this paper, this model is extended to describe heat flow in a double U-tube borehole heat exchanger embedded in an axisymmetric soil mass. Detailed mathematical formulation of the double U-tube together with eigenvalue determination and spectral analysis are given. The mathematical formulation and solution of heat flow in the soil mass are adopted from Al-Khoury [16] but, for completeness, the general solution is described in this paper. The proposed model is utilized to simulate a thermal response test (TRT).

1
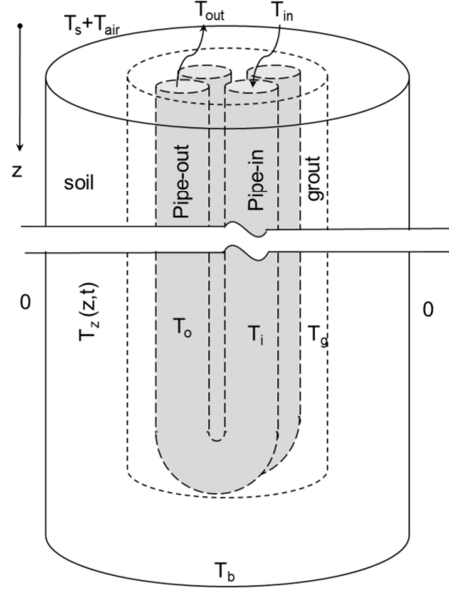
Figure 1. A schematic representation of the double U-tube BHE temperature.

2. Heat flow in the double U-tube borehole heat exchanger

Consider a double U-tube BHE, consisting of five components (two pipes-in, denoted as $i1$ and $i2$; two pipes-out, denoted as $o1$ and $o2$; and grout, denoted as g), see Figure 1. Due to the slenderness of the BHE, the heat flow is considered to occur only along its axial axis. Radial distribution of temperature is in effect negligible. Though, there is heat exchange across the surface areas of the BHE components. Accordingly, the transient heat flow in the BHE components can be expressed as [17]:

Pipes-in

$$\rho c_r \frac{\partial T_{i1}}{\partial t} dV_{i1} - \lambda_r \frac{\partial^2 T_{i1}}{\partial z^2} dV_{i1} + \rho c_r u \frac{\partial T_{i1}}{\partial z} dV_{i1} = b_{ig1}(T_{i1} - T_g) dS_{i1}$$

$$\rho c_r \frac{\partial T_{i2}}{\partial t} dV_{i2} - \lambda_r \frac{\partial^2 T_{i2}}{\partial z^2} dV_{i2} + \rho c_r u \frac{\partial T_{i2}}{\partial z} dV_{i2} = b_{ig2}(T_{i2} - T_g) dS_{i2}$$

(1)

Pipes-out

$$\rho c_r \frac{\partial T_{o1}}{\partial t} dV_{o1} - \lambda_r \frac{\partial^2 T_{o1}}{\partial z^2} dV_{o1} - \rho c_r u \frac{\partial T_{o1}}{\partial z} dV_{o1} = b_{og1}(T_{o1} - T_g) dS_{o1}$$

$$\rho c_r \frac{\partial T_{o2}}{\partial t} dV_{o2} - \lambda_r \frac{\partial^2 T_{o2}}{\partial z^2} dV_{o2} - \rho c_r u \frac{\partial T_{o2}}{\partial z} dV_{o2} = b_{og2}(T_{o2} - T_g) dS_{o2}$$

(2)

Grout

4

1

$$\rho_g c_g \frac{\partial T_g}{\partial t} dV_g - \lambda_g \frac{\partial^2 T_g}{\partial z^2} dV_g = b_{ig1}(T_g - T_{i1})dS_{i1g} + b_{ig2}(T_g - T_{i2})dS_{i2g} +$$

$$b_{og1}(T_g - T_{o1})dS_{o1g} + b_{og2}(T_g - T_{o2})dS_{o2g}$$

(3)

2 in which the subscripts r and g represent the circulating fluid (refrigerant) and the grout,
3 respectively; T_i, T_o and T_g are the temperatures at pipe-in, pipe-out and grout, respectively; λ_r and
4 λ_g are the thermal conductivity of the circulating fluid and grout, respectively; u (m/s) is the
5 circulating fluid velocity; b_{ig} (W/m^2.K) is the reciprocal of the thermal resistance between pipe-in
6 and grout; b_{og} (W/m^2.K) is the reciprocal of the thermal resistance between pipe-out and grout;
7 and ρc (J/ m^3 K) is the volume heat capacity with c (J/kg.K) the specific heat and ρ (kg/m^3) the
8 mass density. dV_{i1} is the partial volume of pipe-in(1), etc. and dS_{i1} is the partial surface area of
9 pipe-in(1), etc.

10 In practice, all U-tube pipes are made of the same materials and have the same size. This entails
11 that heat flow in pipe-in(1) is similar to pipe-in(2) and pipe-out(1) is similar to pipe-out(2),
12 leading to a reduced governing equations, which can be described as

13 **Pipe-in**

14

$$\rho c \frac{\partial T_i}{\partial t} dV_i - \lambda \frac{\partial^2 T_i}{\partial z^2} dV_i + \rho c u \frac{\partial T_i}{\partial z} dV_i = b_{ig}(T_i - T_g)dS_i$$

(4)

15

16 **Pipe-out**

17

$$\rho c \frac{\partial T_o}{\partial t} dV_o - \lambda \frac{\partial^2 T_o}{\partial z^2} dV_o - \rho c u \frac{\partial T_o}{\partial z} dV_o = b_{og}(T_o - T_g)dS_o$$

(5)

18 **Grout**

19

$$\rho_g c_g \frac{\partial T_g}{\partial t} dV_g - \lambda_g \frac{\partial^2 T_g}{\partial z^2} dV_g = 2b_{ig}(T_g - T_i)dS_{ig} + 2b_{og}(T_g - T_o)dS_{og}$$

(6)

20 where the subscript r has been removed for clarity of notation. Note that the grout in Eq. 6 is in
21 contact with two pipes-in and two pipes-out.

22 The associated initial and boundary conditions are typically:

$$T_i(z,0) = T_o(z,0) = T_g(z,0) = T_s(z,0)$$

$$T_i(0,t) = T_{in}(t)$$

23 $$T_i(L,t) = T_o(L,t)$$ (7)

$$-\lambda_g \frac{\partial T_g(z,t)}{\partial z} dS_{gs} - 2b_{ig}(T_g - T_i)dS_{ig} - 2b_{og}(T_g - T_o)dS_{og} = b_{gs}(T_g - T_z)dS_{gs}$$

24 where, initially, the temperature distribution in the BHE components is equal to that of the steady
25 state condition of the soil before heating/cooling operation start. T_{in} is the fluid temperature at z =
26 0, coming from the heat pump; T_z is the soil temperature immediately surrounding the BHE; and
27 b_{gs} is the reciprocal of the thermal resistance between the soil and the grout. dS_{ig}, dS_{og} and dS_{gs} are
28 the partial surface areas at the contact between pipe-in and grout, pipe-out and grout, and grout
29 and soil, respectively.

2.1 Spectral analysis

Integral transform methods are central among many currently applied exact solution techniques for solving transient initial and boundary value problems. The Laplace transform is one of the best known and most widely used integral transform technique. It is utilized to produce an easily solvable ordinary differential equation from a partial differential equation by transforming it from a certain domain, usually time, to the Laplace domain. However, in most cases, finding the inverse transform, which is needed to reconstruct the time function back from the Laplace domain, is quite difficult, if possible, and usually numerical and asymptotic schemes are employed in order to extract usable solutions.

The spectral analysis method, on the other hand, is an important alternative to the Laplace transform for solving many transient problems [18]. It is commonly utilized to transform partial differential equations in time domain to ordinary differential equations in frequency domain and vice versa. Spectral analysis of a space-time function entails discretizing the dependent variables in the frequency domain using the well-known fast Fourier transform algorithm (FFT) and discretization in the spatial domain using Fourier series expansion. It involves solving a homogeneous eigenfunction of the system to obtain its eigenvalues. The general solution of the system can then be obtained economically by summing over all significant eigenvalues, to reconstruct the spatial distribution, and the inverse fast Fourier transform algorithm (IFFT), to reconstruct the temporal distribution.

Using the discrete Fourier transform, a temperature function of time can be discretized as

$$T(z,t_m)=\sum_n \hat{T}(z,\omega_n)e^{i\omega_n t_m}\ , \qquad \hat{T}(z,\omega_n)=\frac{1}{N}\sum_m T(z,t_m)e^{-i\omega_n t_m} \tag{8}$$

in which N is the number of the discrete samples, where, in the fast Fourier transform, it is usually made $N=2^\gamma=2,4,8,\cdots,2048,\cdots$. For a real signal, such as the one treated in this work, the transform is symmetric about a middle frequency, referred to as the Nyquist frequency. This means that N real points are transformed into $N/2$ complex points. For clarity of notation, the summation, the exponential term and the subscripts are ignored and the transform is represented as $T\Leftrightarrow\hat{T}$.

Applying Eq. (8) to Eqs.(4)-(6), gives

$$i\omega\rho c\hat{T}_i dV_i - \lambda\frac{d^2\hat{T}_i}{dz^2}dV_i + \rho cu\frac{d\hat{T}_i}{dz}dV_i - b_{ig}(\hat{T}_i-\hat{T}_g)dS_{ig}=0$$

$$i\omega\rho c\hat{T}_o dV_o - \lambda\frac{d^2\hat{T}_o}{dz^2}dV_o - \rho cu\frac{d\hat{T}_o}{dz}dV_o - b_{og}(\hat{T}_o-\hat{T}_g)dS_{og}=0 \tag{9}$$

$$i\omega\rho_g c_g\hat{T}_g dV_g - \lambda_g\frac{d^2\hat{T}_g}{dz^2}dV_g - 2b_{ig}(\hat{T}_g-\hat{T}_i)dS_{ig} - 2b_{og}(\hat{T}_g-\hat{T}_o)dS_{og}=0$$

where dV_i, dV_o and dV_g are the partial volumes of pipe-in, pipe-out and grout, respectively. In this equation, the spectral representation of the time derivative has been replaced by

$$\frac{\partial T}{\partial t}=\frac{\partial}{\partial t}\sum\hat{T}_n e^{i\omega_n t}=\sum i\omega_n\hat{T}_n e^{i\omega_n t}\Rightarrow i\omega\hat{T} \tag{10}$$

and the spatial derivative is replaced by

1
$$\frac{\partial^m T}{\partial z^m} = \frac{\partial^m}{\partial z^m} \sum \hat{T}_n e^{i\omega_n t} = \sum \frac{\partial^m \hat{T}_n}{\partial z^m} e^{i\omega_n t} \Rightarrow \frac{\partial^m \hat{T}}{\partial z^m} \tag{11}$$

2 The utilization of the spectral approach has reduced the partial differential equations, Eqs. (4)-(6),
3 to ordinary differential equations by converting the time derivative to an algebraic expression.
4 However, the resulting equations are frequency dependent and need to be solved for every
5 frequency ω_n.

6 Collecting terms, Eq. (9) can be written as

7
$$-\lambda \frac{d^2 \hat{T}_i}{dz^2} dV_i + \rho c u \frac{d\hat{T}_i}{dz} dV_i + (i\omega\rho c dV_i - b_{ig} dS_{ig})\hat{T}_i = -b_{ig}\hat{T}_g dS_{ig}$$

$$-\lambda \frac{d^2 \hat{T}_o}{dz^2} dV_o - \rho c u \frac{d\hat{T}_o}{dz} dV_o + (i\omega\rho c dV_o - b_{og} dS_{og})\hat{T}_o = -b_{og}\hat{T}_g dS_{og} \tag{12}$$

$$-\lambda_g \frac{d^2 \hat{T}_g}{dz^2} dV_g + (i\omega\rho_g c_g dV_g - 2b_{ig} dS_{ig} - 2b_{og} dS_{og})\hat{T}_g = -2b_{ig}\hat{T}_i dS_{ig} - 2b_{og}\hat{T}_o dS_{og}$$

8 The associated boundary conditions in the frequency domain are

9
$$\hat{T}_i(0,\omega) = \hat{T}_{in}(\omega)$$

$$\hat{T}_o(L,\omega) = \hat{T}_i(L,\omega) \tag{13}$$

$$-\lambda_g \frac{d\hat{T}_g(z,\omega)}{dz} dS_{gs} - 2b_{ig}(\hat{T}_g - \hat{T}_i)dS_{ig} - 2b_{og}(\hat{T}_g - \hat{T}_o)dS_{og} = b_{gs}(\hat{T}_g - \hat{T}_z(z,\omega))dS_{gs}$$

10 **_Eigenfunction expansion_**

11 The solution of the primary variables can be represented by an exponential complex function of
12 the form [19]:

13
$$\hat{T}_i = A_i e^{-ikz}, \quad \hat{T}_o = A_o e^{ikz}, \quad \hat{T}_g = A_g e^{-ikz} \tag{14}$$

14 in which A_i, A_o, A_g are the integral constants and k denotes the system eigenvalues, which need
15 to be determined. Note that different signs are employed at the exponents of Eq. (14) to impose
16 heat in pipe-in and grout to flow in $z > 0$ direction, and heat in pipe-out to flow in the opposite
17 direction, Figure 1.

18 Substituting Eq. (14) into Eq. (12), rearranging and put in a matrix form, gives

19
$$\begin{pmatrix} \lambda k^2 dV_i - \rho c u i k dV_i + i\omega\rho c dV_i - b_{ig} dS_{ig} & 0 & b_{ig} dS_{ig} \\ 2b_{ig} dS_{ig} & 2b_{og} e^{2ikz} dS_{og} & \lambda_g k^2 dV_g + i\omega\rho c_g dV_g - 2b_{ig} dS_{ig} - 2b_{og} dS_{og} \\ 0 & \lambda k^2 dV_o - \rho c u i k dV_o + i\omega\rho c dV_o - b_{og} dS_{og} & b_{og} e^{-2ikz} dS_{og} \end{pmatrix} \begin{pmatrix} A_i \\ A_o \\ A_g \end{pmatrix} = 0 \tag{15}$$

7

Non-trivial solution of Eq. (15) can only be obtained by letting the determinate equal to zero, giving a complex six degree polynomial of the form:

$$a_6 k^6 + a_5 k^5 + a_4 k^4 + a_3 k^3 + a_2 k^2 + a_1 k + a_0 = 0 \qquad (16)$$

This polynomial represents the eigenfunction of the double U-tube BHE system with k denoting its set of eigenvalues, which can be obtained by solving for the roots of Eq. (16). Only for this set of eigenvalues do the eigenfunction exist that satisfy the boundary conditions of the problem. The exact forms of the coefficients of Eq. (16) are listed in the Appendix.

Six eigenvalues in three complex conjugates are obtained from Eq. (16), representing three basic eigenmodes, one for each BHE component. Accordingly, the solution of the temperature distribution in the three BHE components can be written as

$$\hat{T}_i = A_i e^{-ik_1 z} + B_i e^{-ik_2 z} + C_i e^{-ik_3 z}$$
$$\hat{T}_g = A_g e^{-ik_1 z} + B_g e^{-ik_2 z} + C_g e^{-ik_3 z} \qquad (17)$$
$$\hat{T}_o = A_o e^{ik_1 z} + B_o e^{ik_2 z} + C_o e^{ik_3 z}$$

where the integral constants, $A_i, A_o, \cdots, C_g$ need to be determined from the boundary conditions. Since T_i, T_g, and T_o are coupled, the integral constants, $A_i, A_o, \cdots, C_g$, are related to each other. Eq. (17) can be written as

$$\begin{pmatrix} Q_{11} & 0 & Q_{13} \\ Q_{21} & Q_{22} & Q_{23} \\ 0 & Q_{32} & Q_{33} \end{pmatrix} \begin{pmatrix} A_i \\ A_o \\ A_g \end{pmatrix} = 0 \qquad (18)$$

Following this equation, the relationship between the pipe-in constant and the grout constant can be expressed as

$$A_g = A_{ig} = -\frac{Q_{11}}{Q_{13}} A_i = Y_{ig} A_i \qquad (19)$$

Similarly, the relationship between the pipe-out constant and the grout constant can be expressed as

$$A_g = A_{og} = -\frac{Q_{32}}{Q_{33}} A_o = Y_{og} A_o \qquad (20)$$

For each k there is a corresponding Y_{ig} and Y_{og}, i.e. there is Y_{ig1}, Y_{og1} for k_1, etc. (Doyle, 1988).

Eq. (18) states that there is a direct contact between pipe-in and the grout, and between pipe-out and the grout. There is no direct contact between the two pipes, but the grout works as the medium that transfers heat between them. The contact between pipe-in and pipe-out takes place only at the bottom of the borehole, which is not apparent in this equation. Upon solving this equations, this relatively weak coupling often leads to the generation of a spurious unphysical eigenvalue pair. This eigenvalue pair is too large compared to the other two pairs. This problem is typically encountered in solving transport phenomena using the spectral analysis method, and has been intensively treated in literature (see [20]). To obtain a solution, the spurious eigenvalues

1 have to be eliminated. One of the methods to eliminate the spurious eigenvalues is the reduction
2 of the number of the governing coupled equations.

3 Considering the geometry of the U-tube, where pipe-in meets with pipe-out at the bottom
4 boundary of the borehole, the three coupled differential equations (Eqs. (4)-(6)) can be reduced to
5 two systems of two differential equations plus an algebraic constraint linking the two zones of the
6 grout, as

7 **Pipe-in – grout**

8
$$
\hat{T}_i = A_i e^{-ik_1 z} + B_i e^{-ik_2 z}
$$
$$
\hat{T}_{gi} = A_{ig} e^{-ik_1 z} + B_{ig} e^{-ik_2 z}
$$
(21)

9 **Pipe-out – grout**

10
$$
\hat{T}_o = A_o e^{ik_1 z} + B_o e^{ik_2 z}
$$
$$
\hat{T}_{go} = A_{og} e^{-ik_1 z} + B_{og} e^{-ik_2 z}
$$
(22)

11 and

12
$$
\hat{T}_g = \frac{1}{2}\left(\hat{T}_{gi} + \hat{T}_{go}\right)
$$
(23)

13 This system is governed by the first two eigenvalues.

14 ***Heat flow in Pipe-in – grout***

15 Boundary conditions relevant to Eq. (21) are:

16
$$
\hat{T}_i(0,\omega) = \hat{T}_{in}(\omega)
$$
$$
-\lambda_g \frac{d\hat{T}_{gi}(z,\omega)}{dz} dS_{gs} - 2b_{ig}(\hat{T}_{gi}(z,\omega) - \hat{T}_i(z,\omega))dS_{ig} = b_{gs}(\hat{T}_g(z,\omega) - \hat{T}_z(z,\omega))dS_{gs}
$$
(24)

17 Substituting Eq. (21) into Eq. (24), after rearranging, gives

18
$$
A_i + B_i = \hat{T}_{in}
$$
$$
A_{ig} e^{-ik_1 z}(ik_1\lambda_g dS_{gs} - 2b_{ig} dS_{ig} - b_{gs} dS_{gs}) +
$$
$$
B_{ig} e^{-ik_2 z}(ik_2\lambda_g dS_{gs} - 2b_{ig} dS_{ig} - b_{gs} dS_{gs}) +
$$
$$
2b_{ig} A_i e^{-ik_1 z} dS_{ig} + 2b_{ig} B_i e^{-ik_2 z} dS_{ig} = -b_{gs}\hat{T}_z(z,\omega)dS_{gs}
$$
(25)

19 Using Eq. (19) leads, after rearrangement, to

20
$$
A_i + B_i = \hat{T}_{in}
$$
$$
A_i e^{-ik_1 z}\left[Y_{ig1}(ik_1\lambda_g dS_{gs} - 2b_{ig} dS_{ig} - b_{gs} dS_{gs}) + 2b_{ig} dS_{ig}\right] +
$$
$$
B_i e^{-ik_2 z}\left[Y_{ig2}(ik_2\lambda_g dS_{gs} - 2b_{ig} dS_{ig} - b_{gs} dS_{gs}) + 2b_{ig} dS_{ig}\right] = -b_{gs}\hat{T}_z(z,\omega)dS_{gs}
$$
(26)

21 Putting Eq. (26) in a matrix format, and upon inversing and solving, it can be written as

9

$$A_i = \frac{1}{\Delta_i}\left[a_1 \hat{T}_{\text{in}}(\omega) - \hat{T}_z(z,\omega)\right]$$

$$B_i = \frac{1}{\Delta_i}\left[a_2 \hat{T}_{\text{in}}(\omega) + \hat{T}_z(z,\omega)\right]$$

(27)

in which

$$a_1 = -\frac{e^{-ik_2 z}}{b_{gs}\,dS_{gs}}\left[2b_{ig}\,dS_{ig} + Y_{ig2}(ik_2\lambda_g\,dS_{gs} - 2b_{ig}\,dS_{ig} - b_{gs}\,dS_{gs})\right]$$

$$a_2 = \frac{e^{-ik_1 z}}{b_{gs}\,dS_{gs}}\left[2b_{ig}\,dS_{ig} + Y_{ig1}(ik_1\lambda_g\,dS_{gs} - 2b_{ig}\,dS_{ig} - b_{gs}\,dS_{gs})\right]$$

(28)

and the determinant is:

$$\Delta_i = \frac{e^{-ik_1 z}}{b_{gs}\,dS_{gs}}(2b_{ig}\,dS_{ig} + Y_{ig1}(ik_1\lambda_g\,dS_{gs} - 2b_{ig}\,dS_{ig} - b_{gs}\,dS_{gs})) -$$

$$\frac{e^{-ik_2 z}}{b_{gs}\,dS_{gs}}(2b_{ig}\,dS_{ig} + Y_{ig2}(ik_2\lambda_g\,dS_{gs} - 2b_{ig}\,dS_{ig} - b_{gs}\,dS_{gs}))$$

(29)

Heat flow in Pipe-out – grout

The boundary conditions relevant to Eq. (22) are:

$$\hat{T}_o(L,\omega) = \hat{T}_i(L,\omega) = \hat{T}_{iL}$$

$$-\lambda_g \frac{d\hat{T}_{go}(z,\omega)}{dz}dS_{gs} - 2b_{og}(\hat{T}_{go}(z,\omega) - \hat{T}_o(z,\omega))dS_{og} = b_{gs}(\hat{T}_g(z,\omega) - \hat{T}_z(z,\omega))dS_{gs}$$

(30)

Substituting Eq. (22) into Eq. (30), after rearranging, gives

$$A_o e^{ik_1 L} + B_o e^{ik_2 L} = \hat{T}_{iL}$$

$$A_{og}e^{-ik_1 z}(ik_1\lambda_g dS_{gs} - 2b_{og}dS_{og} - b_{gs}dS_{gs}) +$$

$$B_{og}e^{-ik_2 z}(ik_2\lambda_g dS_{gs} - 2b_{og}dS_{og} - b_{gs}dS_{gs}) +$$

$$2A_o e^{ik_1 z}b_{og}dS_{og} + 2B_o e^{ik_2 z}b_{og}dS_{og} = -b_{gs}dS_{gs}\hat{T}_z(z,\omega)$$

(31)

Using Eq. (20) leads, after rearrangement, to

$$A_o e^{ik_1 L} + B_o e^{ik_2 L} = \hat{T}_{iL}$$

$$A_o e^{-ik_1 z}\left[2e^{2ik_1 z}b_{og}dS_{og} + Y_{og1}(ik_1\lambda_g dS_{gs} - 2b_{og}dS_{og} - b_{gs}\,dS_{gs})\right] +$$

$$B_o e^{-ik_2 z}\left[2e^{2ik_2 z}b_{og}dS_{og} + Y_{og2}(ik_2\lambda_g dS_{gs} - 2b_{og}dS_{og} - b_{gs}dS_{gs})\right] = -b_{gs}dS_{gs}\hat{T}_z(z,\omega)$$

(32)

Putting Eq. (32) in a matrix format, and upon inversing and solving, it can be written as

10

$$A_o = \frac{1}{\Delta_o}\left[b_1\hat{T}_{iL} - e^{ik_2 L}\hat{T}_z(z,\omega)\right]$$

$$B_o = \frac{1}{\Delta_o}\left[b_2\hat{T}_{iL} + e^{ik_1 L}\hat{T}_z(z,\omega)\right] \tag{33}$$

in which

$$b_1 = -\frac{e^{-ik_2 z}}{b_{gs}dS_{gs}}\left[2e^{2ik_2 z}b_{og}dS_{og} + Y_{og2}(ik_2\lambda_g dS_{gs} - 2b_{og}dS_{og} - b_{gs}dS_{gs})\right]$$

$$b_2 = \frac{e^{-ik_1 z}}{b_{gs}dS_{gs}}\left[2e^{2ik_1 z}b_{og}dS_{og} + Y_{og1}(ik_1\lambda_g dS_{gs} - 2b_{og}dS_{og} - b_{gs}dS_{gs})\right] \tag{34}$$

and the determinant is

$$\Delta_o = \frac{e^{-ik_1 z}}{b_{gs}dS_{gs}}\left[2e^{2ik_1 z}b_{og}dS_{og} + Y_{og1}(ik_1\lambda_g dS_{gs} - 2b_{og}dS_{og} - b_{gs}dS_{gs})\right]e^{ik_2 L} -$$

$$\frac{e^{-ik_2 z}}{b_{gs}dS_{gs}}\left[2e^{2ik_2 z}b_{og}dS_{og} + Y_{og2}(ik_2\lambda_g dS_{gs} - 2b_{og}dS_{og} - b_{gs}dS_{gs})\right]e^{ik_1 L} \tag{35}$$

General solution of BHE heat equations

Having determined the eigenvalues and the integration constants, the general solution of the double U-tube BHE system of equations can then be obtained by summing over all eigenfunctions (corresponding to k_1 and k_2) and frequencies, as

Pipe-in – grout

$$T_i(z,t) = \sum_n \left(A_i e^{-ik_1 z} + B_i e^{-ik_2 z}\right)e^{i\omega_n t} \tag{36}$$

Pipe-out – grout

$$T_o(z,t) = \sum_n \left(A_o e^{ik_1 z} + B_o e^{ik_2 z}\right)e^{i\omega_n t} \tag{37}$$

Grout

$$T_g(z,t) = \frac{1}{2}\sum_n \left[\left(Y_{ig1}A_i + Y_{og1}A_o\right)e^{-ik_1 z} + \left(Y_{ig2}B_i + Y_{og2}B_o\right)e^{-ik_2 z}\right]e^{i\omega_n t} \tag{38}$$

where A_i and B_i are defined in Eq. (27), A_o and B_o are defined in Eq. (33), $Y_{ig1}...Y_{og2}$ are defined in Eqs. (19)-(20) and k_1 and k_2 are determined from solving the roots of Eq. (16). The reconstruction of the time domain is obtained using inverse FFT algorithm.

3. Heat flow in the soil mass

A detailed derivation of heat flow in the soil mass is given in Al-Khoury [16,17]. Following that, the general solution of the soil heat equations in the time domain can be expressed as

$$T_{\text{soil}}(r,z,t) = T_{st}(z) + T_{tr}(z,t) + T_{rz}(r,z,t) \tag{39}$$

in which

11

$$T_{st}(z) = T_s\left(1 - \frac{z}{h}\right) + T_b\frac{z}{h} \tag{40}$$

$$T_{tr}(z,t) = \sum_n\left(-\frac{\Delta\hat{T}(\omega)}{1 - e^{-2\kappa_n h}}e^{\kappa_n(z-2h)} + \frac{\Delta\hat{T}(\omega)}{1 - e^{-2\kappa_n h}}e^{-\kappa_n z}\right)e^{i\omega_n t} \tag{41}$$

and

$$T_{rz}(r,z,t) = \sum_n\sum_m A_m J_0(\xi_m r)e^{i\omega_n t} \tag{42}$$

where

$$\kappa = \sqrt{i\omega/\alpha}$$
$$\zeta = (-\kappa^2 - \xi^2)^{1/2}$$
$$\xi_m = \frac{\beta_m}{R} \tag{43}$$
$$A_m = -\frac{i(e^{-i\zeta_m L} - 1)}{\zeta_m L(-i\zeta_m\lambda_s + b_{gs})}b_{gs}\hat{T}_g(z)$$

4. Reconstructing the Thermal Response Test data

The proposed spectral analysis model has been implemented in a computer code, SA-Geotherm, developed at Delft University of Technology. Both single and double U-tubes borehole heat exchangers embedded in an axisymmetric soil mass are implemented. In [15,16] full verification examples were given for heat flow in a single U-tube BHE embedded in a soil mass. Here, we examine the double U-tube BHE and its thermal interaction with the soil mass by reconstructing a real thermal response test data.

Thermal Response Test (TRT) is an in-situ parameter identification experiment for the characterization of ground thermal properties, Figure 2. It is one of the most utilized technique for determining the thermal conductivity of soil and the borehole thermal resistance.

Several analytical and numerical models have been utilized for the interpretation of TRT test results. The infinite line source model has been utilized by, among others, Mogensen [21], Hellström [22], Gehlin [23]; the finite line source model by Bandos et al. [24], to give only few examples. Numerical models have been utilized by, among others, Signorelli et al. [25], Zanchini [26], and Schiavi [27]. Nevertheless, the line source model is widely utilized for this purpose because of its simplicity of use. However, this model suffers from several shortcomings. Among others, it lumps all convective-conductive heat flow in the U-tubes and grout and their thermal interactions together with their geometry and material properties into a constant conductive infinite line source. Apparently, this simplification is a rather simplistic representation of the physics of the problem.

Here, we utilize the proposed spectral model to simulate the TRT and to back calculate the soil thermal conductivity.

Figure 2. TRT equipment

TRT case study

The thermal response test was carried out in Emilia Romagna region in Italy. The borehole heat exchanger is 100 m in length and 0.127 m in diameter with a filling grout made of bentonite. The collector is a double U-tube with an external diameter of 0.032 m. The working fluid is water.

The stratigraphy of the area is:

- 0 to 1.5 m: dry clay.
- 1.5 to 100 m: marl (there are some small infiltrations of water between 60 and 65 m depths).

Due to this simple stratigraphy, the soil formation surrounding the borehole was considered to be consisting of a single layer. The physical and material parameters of the soil formation and the TRT borehole are given in Table 1. The averaged soil thermal conductivity is not shown in the table because it needs to be determined.

During the experiment, the fluid volume flow was measured, together with the inlet and outlet temperatures. No real insulation was made to the upper part of the BHE. The experiment was conducted in a cooling mode, i.e. injection of heat into the ground. Figure 3 shows the measured inlet and outlet temperatures versus time.
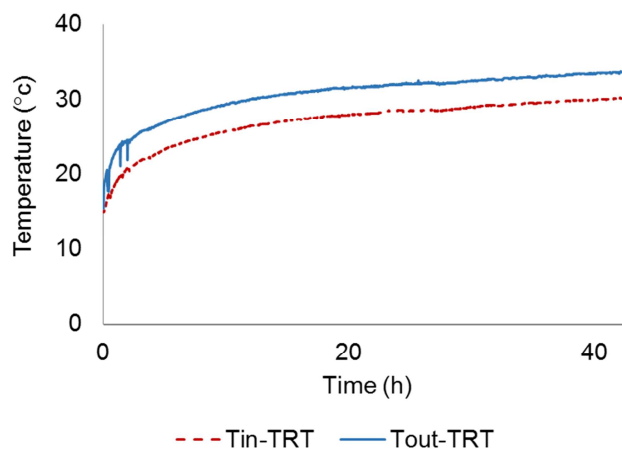
Figure 3. Measured inlet and outlet temperatures during TRT.

1 <div align="center">Table 1. Physical and material parameters</div>

Parameter	Value
Borehole:	
Borehole length	100 m
Borehole diameter	0.127 m
Pipe external diameter	0.032 m
Pipe thermal conductivity	0.42 W/(mK)
Fluid:	
Fluid thermal conductivity	0.56 W/(mK)
Fluid dynamic viscosity	0.001 Pa.s
Fluid velocity	0.42 m/s
Fluid specific thermal capacity	4180 J/(kg.K)
Grout:	
Grout density	1420 kg/m^3
Grout thermal conductivity	0.6 W/(m.K)
Grout specific thermal capacity	1197 J/(kg.K)
Soil:	
Soil specific thermal capacity	400 J/(kg.K)
Soil density	1680 kg/m^3

2

3 *Computational procedure*

4 In this work, no attempt was made to conduct inverse calculations by a minimization of an
5 objective function. (This will be carried out in a forthcoming work.) Rather, several spectral
6 analyses were conducted by keeping all parameters fixed, but varying the soil thermal
7 conductivity, until there is a match between the experimental results and the computed ones.

8 Time discretization of T_{in} and T_{air} signals was conducted using the forward FFT algorithm. The
9 number of samples was 16,384 (2^{14}) and the sample length was 30 s, giving a time window of
10 approximately 136 hours. Spatial discretization of the soil mass was conducted using 100 Bessel
11 function roots, and the far field boundary of the region-of-interest R was calculated as

$$R = \sqrt{6\alpha t} \qquad (44)$$

13 where α is the thermal diffusivity of the soil and t is the time when the temperature at point R
14 reaches its maximum [1]. In this work t was set equal to 100 days, giving R approximately 12 m.
15 A discussion on this choice is given in [16].

16 The thermal resistance coefficients between the borehole components and between the borehole
17 and the soil mass are calculated using the Y-configuration analogy to Ohm's law [17]. Following
18 this configuration, heat transfer coefficients for pipe-in - grout and pipe-out - grout can described
19 as

$$b_{ig} = \frac{1}{R_{ig}}; \quad b_{og} = \frac{1}{R_{og}} \qquad (45)$$

where

$$R_{ig} = R_{\text{convection}} + R_{\text{pipe material}} = \frac{1}{r_o/r_i\,\bar{h}} + \frac{r_o\ln(r_o/r_i)}{\lambda_p} \tag{46}$$

in which r_i and r_o are the inner and outer radius of pipe-in, respectively; λ_p is the thermal conductivity of pipe-in material; and $\bar{h} = \text{Nu}\lambda/D$ is the convective heat transfer coefficient, where D is the inner diameter of the pipe and Nu is the Nusselt Number of the circulating fluid. A similar formulation is valid for R_{og}.

Heat transfer coefficient of the grout-soil is described as

$$b_{gs} = \frac{1}{2R_{ig} + 2R_{og} + R_{gs}} \tag{47}$$

where

$$R_{gs} = \frac{r_g\ln(r_g/r_{eq})}{\lambda_g} \tag{48}$$

in which r_g is the radius of the grout (borehole), and $r_{eq} = 2\sqrt{r_{\text{in}}^2 + r_{\text{out}}^2}$ with r_{in} is pipe-in inner radius and r_{out} is pipe-out inner radius.

Input parameters

The computer code requires description of the geometry, material parameters and initial and boundary conditions of both, the BHE and the soil mass. The geometry parameters include information about the dimensions of the BHE components. The material parameters include information about the thermal properties of the BHE components and the soil mass. The initial condition includes the BHE and soil initial temperatures. The boundary conditions include the input temperature at the inlet of pipe-in, together with the flow rate of the circulating fluid, and the air temperature at the soil mass surface.

Not all information necessary to be input into the code were recorded during the experiment. Though, estimates could be deduced from the available measurements. The initial temperature in the soil and the borehole were assumed similar to T_{in} at the beginning, i.e. 13 °C. During the experiment, the air temperature was varying between 13 and 20 °C. Table 2 shows the air temperature variation with time, as was input in the code. The geometry and the material parameters were input as those given in Table 1.

Table 2. Input air temperature

Time (h)	Air temperature (°C)
0	13
0.1	13.5
0.3	14
0.6	15
1.4	17
2.8	19

| 4.2	20
21	20
40	18
45	16

Computational results

As mentioned above, the backcalculation of the soil thermal conductivity was conducted by performing several calculations with varying soil thermal conductivity. The best fit solution is shown in Figure 4, where the soil thermal conductivity was equal to 2.15 W/m K. The figure shows the measured T_{in} and T_{out} together with the computed T_{out}.

Apparently, the results are close and the model is capable of reconstructing the TRT in the long and short terms, as shown on the left and right hand sides of the figure respectively. An important feature of the model is manifested on the right hand side figure. The measured spikes in T_{in} data are shifted in time in the measured T_{out} data and exhibited damping. The computed T_{out} accurately exhibits these two occurrences.

In addition to reconstructing the TRT measured data at pipe-in inlet and pipe-out outlet, the model is capable of computing the temperature distribution at any point along the borehole and in the soil mass. For example, Figure 5 shows, in addition to pipe-in and pipe-out, the temperature distribution of the grout at the borehole surface. Figure 6 shows the temperature distribution of the soil at different radial distances from the borehole at $z = 0.25$ m.
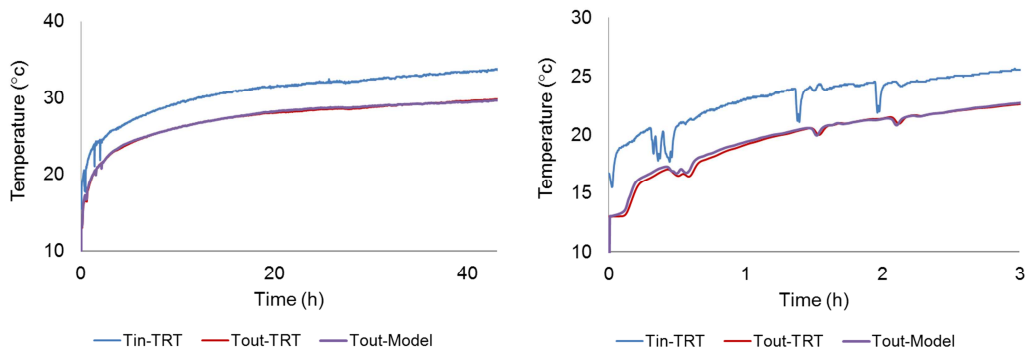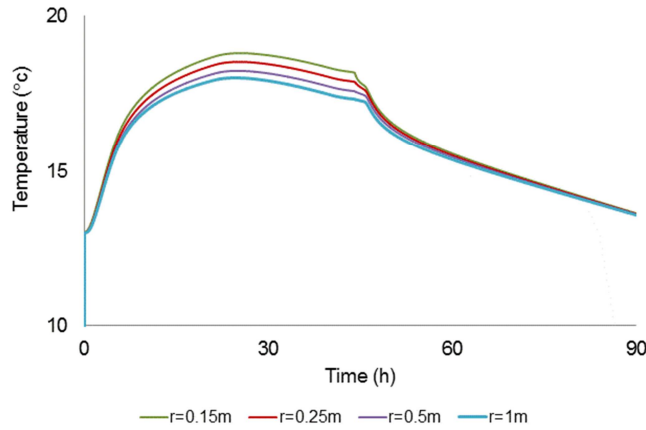
Figure 4. Best match of the TRT data, obtained with soil thermal conductivity equal to 2.15 W/mK.
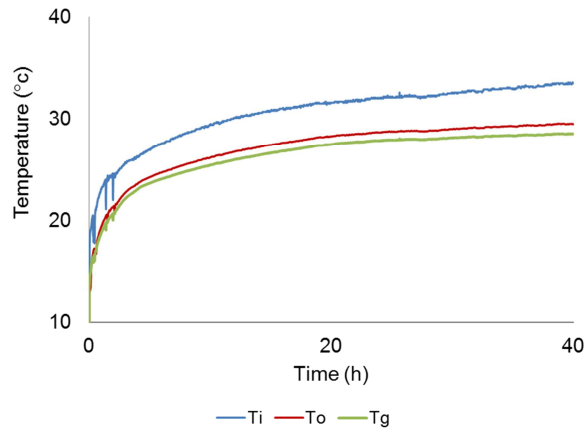
Figure 5. Temperature vs. time of pipe-in, pipe-out and grout at z = 0 m.

Figure 6. Soil temperature vs. time at different radial distances from the center of the borehole at depth = 0.25 m

Discussion

The TRT results were utilized to validate the capability of the proposed spectral model to simulate heat flow in a double U-tube borehole heat exchanger and its thermal interaction with the surrounding soil mass. Two outcomes can be deduced from this case study: 1. Accuracy, and 2. Computational efficiency.

For the first, the comparison between the experimental results and the computed shows that the model is accurate for both, the short term and the long term. As shown in Figure 4, details of the response in the short term are accurately captured by the model. In the long term, the computed results are very much matching those of the experiment.

For the second, the proposed spectral model shares the simplicity of use of the infinite line source model, but strongly overrules it in simulating the physics of the problem. This model is capable of simulating full conductive-convective heat flow in all BHE components and their thermal interactions between themselves and between the BHE and the soil mass. All geometrical and material properties are taken into consideration.

17

1　The gained computational accuracy and efficiency of the proposed model make it suitable for an
2　appropriate inverse calculation based on minimization of objective functions describing the
3　difference between the experimental results and the computed. Such an inverse model is currently
4　under development.

5　## 5. Parametric analyses

6　Having reconstructed the TRT experimental result, a parametric analysis was conducted to study
7　the effect of different material and physical parameters on heat flow in the system. Thermal
8　conductivity of the soil was kept constant. The following was studied:

9　**Grout thermal conductivity**: Figure 7 shows the temperature distribution vs. time at the outlet of
10　pipe-out for different grout thermal conductivity: $\lambda g = 0.4, 0.6, 1.0$ and 10.0 W/m.K. The figure
11　shows that the effect of this parameter, for this set up, is not negligible.

12　This example represents a cooling mode; i.e. water with a temperature greater than that of the soil
13　is inject at the inlet of pipe-in. In spite of this, the calculated fluid temperature at the outlet is
14　higher for the high grout conductivity. This is attributed to that for a high grout conductivity,
15　more heat transfers from the inlet to the outlet via the grout; while for a low grout conductivity,
16　the opposite occurs. As heat transfer in the U-tube is mostly convective, thermal resistance
17　between the pipes and the grout is small, allowing more heat to transfer between the BHE
18　components, as compared to the conductive heat transfer between the BHE and the surrounding
19　soil. This phenomenon cannot be captured by models based on averaging the temperatures in
20　pipe-in and pipe-out and ignoring the thermal resistance and the convective heat transfer along
21　the U-tube length.

22　This issue seems in contradiction with the common practice which promotes the utilization of
23　grout with more conductivity at all times. In fact, this should not be the case. In the heating mode,
24　for instance, we tempt to gain more heat while the working fluid is running along pipe-in; and
25　preserve the gained heat while the fluid is running through pipe-out. Using high conductivity
26　grout would allow gaining more heat along pipe-in, but on the other hand, losing more heat along
27　pipe-out. Therefore, there should be an appraisal on how much heat needs to be gained and lost.
28　This should be made at the design level, depending on the initial and boundary conditions,
29　together with the required geometry and physical parameters.
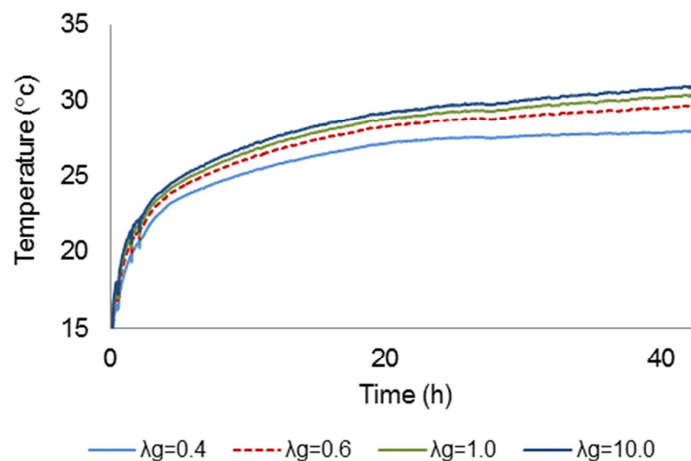
30
31　Figure 7. Temperature distribution of Tout for different grout thermal conductivity.

18

1   **Injection flow rate**: Figure 8 shows the temperature distribution vs. time at the outlet of pipe-out
2   for different fluid velocity: u = 0.21, 0.42 and 0.84 m/s. The figure shows that this parameter, in
3   the studied range, is not negligible. With higher velocity, there is a less time for the thermal
4   interaction between the BHE and the soil, and hence higher temperature in the output. However,
5   this is influenced by other factors, such as, the thermal conductivities of the involved components,
6   the viscosity of the working fluid, and the geometry of the BHE. Therefore, during the design
7   process, an appraisal between the heat flow rate and the gained temperature should be made.
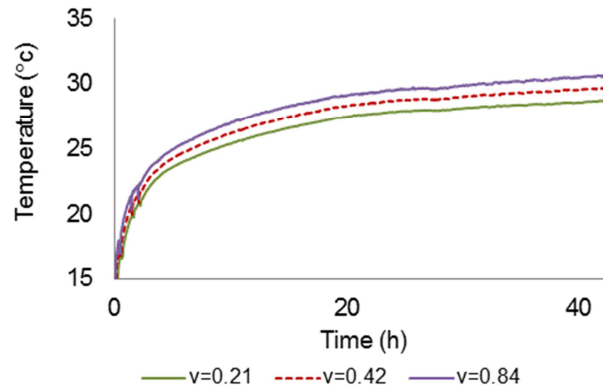
8

9   Figure 8. Temperature distribution of Tout for different injection flow rates.

10   **Fluid viscosity**: Figure 9 shows the temperature distribution vs. time at the outlet of pipe-out for
11   different fluid dynamic viscosity μ = 0.0008, 0.001 and 0.002 Pa.s. The fluid velocity is kept
12   constant. The figure shows that this parameter, in the studied range, has some effect on the heat
13   flow, but its significance would depend on the application. With higher viscosity, the circulating
14   fluid can keep more heat, and hence brings higher temperature to the output.

15
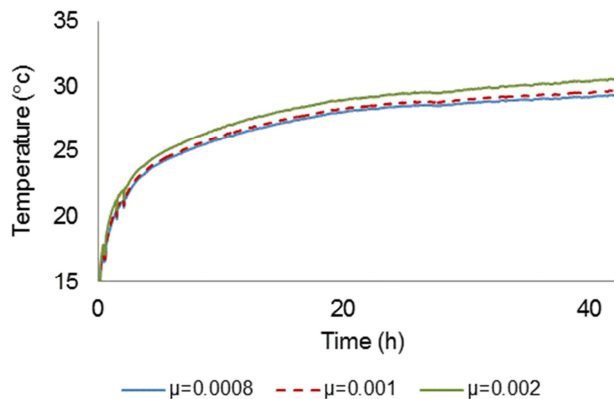
16

17   Figure 9. Computational results of TRT by varying fluid viscosity.

18 **6. Conclusions**

19 A spectral model for the simulation of transient conductive-convective heat transfer in an
20 axisymmetric shallow geothermal system consisting of a double U-tube borehole heat exchanger
21 embedded in a soil mass is introduced. The fast Fourier transform is utilized for the discretization
22 of the governing partial differential equations in the time domain. Complex Fourier and Fourier-

19

Bessel series are utilized for the discretization in the spatial domain. The eigenvalues of the borehole heat exchanger are obtained by eigenfunction expansion, and those of the soil are obtained by prescribing a homogeneous boundary condition at a fictitious boundary at some distance $r = R$, where the effect of the borehole heat exchanger temperature is known a priori to vanish. This condition allows for an algebraic summation over Fourier-Bessel series. This is particularly important because the involved integrands are transcendental and their evaluation using typical semi-infinite contour integration requires, if possible, excessive computational demands.

The proposed model combines the exactness of the analytical methods with a great extent of generality in describing the geometry and boundary conditions of the numerical methods. These features make the model useful in engineering practice. The CPU time for calculating temperature distributions in all involved shallow geothermal system components: pipe-in, pipe-out, grout, and soil; using 16,384 FFT samples, for the time domain, and 100 Fourier-Bessel series samples, for the spatial domain; was in the order of 1 second in an Intel PC.

As a result of the model accuracy and computationally efficiency, it can be utilized in an iterative scheme for parameter identification of soil thermal parameters. In this publication, the model is utilized to back calculate the soil thermal conductivity by comparing its computational results with those obtained from a thermal response test. The backcalculation was conducted manually by performing several calculations until a best fit is obtained. In a forthcoming work, an appropriate inverse model based on minimization of the system objective function will be introduced.

The model can be utilized for forward and inverse calculations of problems related to heat flow in a double U-tube geothermal heat pump system. However, it is valid for a single layer system. For a multilayer system, the model should be formulated within the spectral element method. The spectral element method is a semi-analytical technique combining the exact spectral solution of the system in a homogeneous domain to the finite element method solution of a heterogeneous domain. The development of a spectral element model is currently underway.

7. Appendix

The coefficients of the six-degree polynomial of the double U-tube eigenfunction are:

$$a_6 = \lambda^2 \lambda_g dV_i dV_o dV_g$$

$$a_5 = -2i\lambda\lambda_g \rho cu dV_i dV_o dV_g$$

$$a_4 = -b_{ig}\lambda_g\lambda dS_{ig}dV_gdV_o - \rho^2 c^2 u^2 \lambda_g dV_i dV_g dV_o + 2i\lambda\lambda_g\omega\rho cd dV_i dV_g dV_o - \\ 2\lambda^2 b_{og} dV_i dS_{og} dV_o - \lambda\lambda_g b_{og} dV_i dS_{og} dV_g + i\lambda^2 \omega\rho_g c_g dV_i dV_g dV_o - \\ 2\lambda^2 b_{ig} dV_i dS_{ig} dV_o$$

$$a_3 = 2\rho^2 c^2 u\lambda_g\omega dV_i dV_g dV_o + i\rho cu\lambda_g b_{og} dV_i dV_g dS_{og} + i b_{ig}\lambda_g \rho cu dV_o dV_g dS_{ig} + \\ 4i\lambda b_{og} \rho cu dV_o dV_i dS_{og} + 2\lambda\rho cu\omega\rho_g c_g dV_o dV_i dV_g + 4i\lambda b_{ig}\rho cu dV_o dV_i dS_{ig}$$

20

$$a_2 = 2\lambda b_{ig} b_{og} dV_i dS_{ig} dS_{og} - 4i\lambda b_{ig} \omega\rho c d V_i dV_o dS_{ig} - \omega^2 \rho^2 c^2 \lambda_g dV_i dV_o dV_g -$$
$$ib_{ig} \omega\rho_g c_g \lambda dV_g dV_o dS_{ig} - 2\lambda\omega^2 \rho_g c_g \rho c d V_i dV_o dV_g + 2\rho^2 c^2 u^2 b_{ig} dV_i dV_o dS_{ig} -$$
$$i\omega\rho c \lambda_g b_{og} dV_i dV_g dS_{og} + b_{ig} b_{og} \lambda_g dS_{ig} dV_g dS_{og} + 2\rho^2 c^2 u^2 b_{og} dV_i dV_o dS_{og} +$$
$$2b_{ig} b_{og} \lambda dS_{ig} dV_o dS_{og} - 4i\lambda b_{og} \omega\rho c d V_i dV_o dS_{og} - ib_{ig} \lambda_g \omega\rho c d V_g dV_o dS_{ig} -$$
$$i\lambda\omega\rho_g c_g b_{og} dV_i dV_g dS_{og} - i\rho^2 c^2 u^2 \omega \rho_g c_g dV_i dV_o dV_g$$

$$a_1 = 2i\rho^2 c^2 u\omega^2 \rho_g c_g dV_i dV_o dV_g - 2ib_{ig} b_{og} \rho c u dV_o dS_{ig} dS_{og} - \rho c u \omega \rho_g c_g b_{og} dV_i dV_g dS_{og} -$$
$$4\rho^2 c^2 u\omega b_{ig} dV_i dV_o dS_{ig} - 4\rho^2 c^2 u\omega b_{og} dV_i dV_o dS_{og} - b_{ig} \omega\rho_g c_g \rho c u dV_o dV_g dS_{ig} -$$
$$2i\rho c u b_{ig} b_{og} dV_i dS_{ig} dS_{og}$$

$$a_0 = -i\omega^3 \rho^2 c^2 \rho_g c_g dV_i dV_o dV_g + 2\omega^2 \rho^2 c^2 b_{og} dV_i dV_o dS_{og} + 2\omega^2 \rho^2 c^2 b_{ig} dV_i dV_o dS_{ig} +$$
$$\omega^2 \rho c \rho_g c_g b_{og} dV_i dV_g dS_{og} + 2i\omega\rho c b_{ig} b_{og} dV_i dS_{ig} dS_{og} + 2i\omega\rho c b_{ig} b_{og} dV_o dS_{ig} dS_{og} +$$
$$ib_{ig} \omega\rho_g c_g b_{og} dV_g dS_{ig} dS_{og} + b_{ig} \omega^2 \rho_g c_g \rho c d V_o dV_g dS_{ig}$$

References

[1] Carslaw HS, Jaeger JC. Conduction of Heat in Solids. 2nd edition. Oxford University Press, London, UK: 1959.

[2] Ingersoll LR, Zobel OJ, Ingersoll AC. Heat Conduction with Engineering, Geological, and other Applications. Revised edition. University of Wisconsin press; 1954.

[3] Philippe M, Bernier M, Marchio D. Validity ranges of three analytical solutions to the transfer in the vicinity of single boreholes. Geothermics 2009; 38, 407-413.

[4] Gu Y, O'Neal DL. An Analytical Solution to transient heat conduction in a composite region with a cylindrical heat source. ASME Journal of Solar Energy Engineering 1995; 117, 242-248.

[5] Lamarche L, Beauchamp B. New solutions for the short-time analysis of geothermal vertical boreholes. International Journal of Heat and Mass Transfer 2007; 50, 1408-1419.

[6] Bandyopadhyay G, Gosnold W, Mann M. Analytical and semi-analytical solutions for short-time transient response of ground heat exchangers. Energy and Buildings 2008; 40, 1816-1824.

[7] Marcotte D, Pasquier P. Fast fluid and ground temperature computation for geothermal ground-loop heat exchanger systems. Geothermics 2008; 37, 651-665.

[8] Javed S, Claesson J. New analytical and numerical solutions for the short-term analysis of vertical ground heat exchangers. ASHRAE Transactions 2011; Vol. 117(1): 3-12.

[9] De Carli M, Tonon M, Zarrella A, Zecchin R. A computational capacity resistance model (CaRM) for vertical ground coupled heat exchangers. Renewable Energy 2010; 35, 1537-1550.

[10] Zarrella A, Scarpa M, De Carli M. Short time step analysis of vertical ground-coupled heat exchangers: The approach of CaRM. Renewable Energy 2011; 36, 2357-2367.

[11] Bauer P, Heidemann W, Muller-Steinhagen H, Diersch HJG. Thermal resistance and capacity models for borehole heat exchangers. International Journal of Energy Research 2010; Vol. 35(4), 312-320.

[12] Pasquier P, Marcotte D. Short-term simulation of ground heat exchanger with an improved TRCM. Renewable Energy 2012; 46, 92-99.

[13] Eskilson P and Claesson J. Simulation model for thermally interacting heat extraction boreholes. Numerical Heat Transfer 1988; 13, 149-165.

[14] Zeng H, Diao N, Fang Z. Heat transfer analysis of boreholes in vertical ground heat exchangers. International Journal of Heat and mass Transfer 2003; 46, 4467-4481.

[15] Al-Khoury R. Spectral framework for geothermal borehole heat exchangers, International Journal for Numerical Methods for Heat and Fluid Flow 2010; 20(7), 773-793.

[16] Al-Khoury R. A spectral model for shallow geothermal systems. International Journal for Numerical Methods for Heat and Fluid Flow 2012; 22(1), 49-72.

[17] Al-Khoury R. Computational modeling of shallow geothermal systems. CRC Press/ Taylor & Francis Group; 2012.

[18] Doyle JF. Spectral analysis of coupled thermoelastic waves. Journal of Thermal Stresses 1988; 11, 175-185.

[19] Doyle JF. Wave Propagation in Structures: Spectral Analysis Using Fast Discrete Fourier Transforms. Springer-Verlag, New York; 1997.

[20] Manning ML, Bamieh B, Carlson JM. Descriptor approach for eliminating spurious eigenvalues in hydrodynamic equations. Cornell University Library, arXiv:0705.1542 [physics.comp-ph]; 2008.

[21] Mogensen P. Fluid to Duct Wall Heat Transfer in Duct System Heat Storage. Proc. Int. Conf. On Subsurface Heat Storage in Theory and Practice. Stockholm. Sweden, June 6–8, 1983, 652-657.

[22] Hellström G. Thermal Analysis of Duct Storage System. Dep. of Mathematical Physics University of Lund, Lund, Sweden; 1991, pp. 262.

[23] Gehlin S. Thermal response test. Method, development and evaluation. 2002; Department of Environmental Engineering, University of Lulea, Sweden.

[24] Bandos T, Montero A, Fernández E, Santander JLG, Isidro JM, Pérez J et al.. Finite line-source model for borehole heat exchangers: effect of vertical temperature variations. Geothermics 2009; 38, 263-370.

[25] Signorelli S, Bassetti S, Pahud D, Kohl T. Numerical evaluation of thermal response tests. Geothermics 2007; 36, 141 – 166.

[26] Zanchini E, Terlizzese T. Finite-element evaluation of thermal response tests performed on U-tube borehole heat exchangers. Proceedings of the COMSOL Conference 2008, Hannover, Germany.

[27] Schiavi L. 3D simulation of the Thermal Response Test in a U-tube Borehole Heat Exchanger. Proceedings of the COMSOL Conference 2009, Milan.